REPORTS OF PRACTICAL ONCOLOGY AND RADIOTHERAPY 23 (2018) 183–188

Available online at www.sciencedirect.com

ScienceDirect

journal homepage: http://www.elsevier.com/locate/rpor

Technical note

4D modeling in a gimbaled linear accelerator by using gold anchor markers

Hideharu Miura[a,b,*], *Shuichi Ozawa*[a,b], *Takaaki Matsuura*[a], *Atsushi Kawakubo*[a], *Fumika Hosono*[a], *Kiyoshi Yamada*[a], *Yasushi Nagata*[a,b]

[a] *Hiroshima High-Precision Radiotherapy Cancer Center, Hiroshima, Japan*

[b] *Department of Radiation Oncology, Institute of Biomedical & Health Science, Hiroshima University, Hiroshima, Japan*

ARTICLE INFO

Article history:
Received 11 September 2017
Received in revised form
20 December 2017
Accepted 16 February 2018
Available online 18 March 2018

Keywords:
4D-modeling
Gold anchor marker
IGRT
Image quality
Vero4DRT

ABSTRACT

Purpose: The purpose of this study was to verify whether the dynamic tumor tracking (DTT) feature of a Vero4DRT system performs with 10-mm-long and 0.28 mm diameter gold anchor markers.

Methods: Gold anchor markers with a length of 10 mm and a diameter of 0.28 mm were used. Gold anchor markers were injected with short and long types into bolus material. These markers were sandwiched by a Tough Water (TW) phantom in the bolus material. For the investigation of 4-dimensional (4D) modeling feasibility under various phantom thicknesses, the TW phantom was added at 2 cm intervals (in upper and lower each by 1 cm). A programmable respiratory motion table was used to simulate breathing-induced organ motion, with an amplitude of 30 mm and a breathing cycle of 3 s. X-ray imaging parameters of 80 kV and 125 kV (320 mA and 5 ms) were used. The least detection error of the fiducial marker was defined as the 4D-modeling limitation.

Results: The 4D modeling process was attempted using short and long marker types and its limitation with the short and long types was with phantom thicknesses of 6 and 10 cm at 80 kV and 125 kV, respectively. However, the loss in detectability of the gold anchor because of 4D-modeling errors was found to be approximately 6% (2/31) with a phantom thickness of 2 cm under 125 kV. 4D-modeling could be performed except under the described conditions.

Conclusions: This work showed that a 10-mm-long gold anchor marker in short and long types can be used with DTT for short water equivalent path length site, such as lung cancer patients, in the Vero4DRT system.

* *Corresponding author at*: Hiroshima High-Precision Radiotherapy Cancer Center, 3-2-2, Futabanosato, Higashi-ku, Hiroshima 732-0057, Japan.

E-mail address: miura@hiprac.jp (H. Miura).

https://doi.org/10.1016/j.rpor.2018.02.008

1507-1367/

1. Introduction

Respiratory tumor motion management is one of the most important issues in radiotherapy, especially in the case of thoracic and abdominal tumors.[1] Various methods have been proposed to reduce the impact of respiratory-induced tumor motion during beam delivery. The dynamic tumor tracking (DTT) technique with a gimbal-mounted linac for respiratory-induced tumor motion compensation is capable of tracking the three-dimensional (3D) position of a fiducial marker based on four-dimensional (4D) modeling.[2–4] The Vero4DRT system is in clinical use for respiratory-induced organ motion, such as in the lung, liver, and pancreas. Doses to the planning target volume (PTV) and to organs at risk (OARs) in DTT have been shown to be 30–35% and 20–30% lower than those in conventional motion encompassing methods.[4] Matsuo et al. summarized procedures, the quantify tracking error, tumor-fiducial uncertainties, and PTV margins for DTT at the Kyoto University (KU, Kyoto, Japan), Institute of Biomedical Research and Innovation (IBRI, Kobe, Japan) and UZ Brussel (UZB, Brussels, Belgium). The Vero4DRT system for DTT uses kilo-voltage (kV) X-rays for target localization, but in soft tissues it is not possible to visualize the target on the kV X-ray images. The Vero4DRT system performs DTT using fiducial markers, made of high-Z materials, such as gold, near or in the target. KU-IBRI implanted three or more 1.5 mm spherical gold markers around the tumors using a bronchoscope. UZB inserted a cylindrical 0.75 mm diameter gold marker inside or close to the tumor percutaneously.[3] 0.75 mm diameter Visicoil marker was used in its first clinical application for the treatment of a patient with liver cancer in our institution. Larger fiducial markers need to be inserted with large diameter needles that cause pain. In addition, the presence of metal may influence the dose distribution.[5]

A 0.5%-iron-containing fiducial marker has been shown to be useful in an image registration and bleeding and pain can be avoided by the use of a thin needle.[6] 4D modeling is achieved by detecting the implanted fiducial markers in kV X-ray images acquired before treatment. These implanted fiducial markers require high image contrast for accurate target position information because 4D modeling fails under poor or ambiguous imaging conditions. The physical characteristics of the gold markers strongly depend on their length and diameter.[7–9] The Vero4DRT system for clinical use must anticipate the possibility that detection by the marker or the 4D-modeling may fail. To the best of our knowledge, gold anchor markers have not been reported for use in 4D modeling in the Vero4DRT system.

The purpose of the current study was to verify whether the DTT feature of the Vero4DRT system performs with a gold anchor marker. The feasibility of the gold anchor marker under various phantom thicknesses was investigated using 4D modeling. The detectability loss of the gold anchor marker was quantified, and the limitation of 4D modeling was investigated.

2. Materials and methods

The Vero4DRT system (Mitsubishi Heavy Industries, Ltd., Tokyo, Japan, and Brainlab, Feldkichen, Germany) was used in this work. Mechanical details of the Vero4DRT system have been described elsewhere.[10–15] In brief, DTT is based on the correlation between the internal tumor position and external surrogated infrared (IR) markers. This is known as 4D modeling. The 3D positions of the internal target are provided via an implanted fiducial marker detected with the kV X-ray imaging subsystems. These orthogonal systems are attached to the O-ring at 45° from the mega voltage (MV) beam axis. The gimbal swinging pursues the target in real time for organ motion compensation of the treatment beam along two orthogonal directions (pan and tilt) up to ±2.5°, based on 4D modeling. Two types of fiducial markers are available with the Vero4DRT system: a spherical (short type) and cylindrical (long type) marker. The gold anchor marker had a winding, zigzag shape that could be bent into a spherical shape. Gold anchor markers with a length of 10 mm and a diameter of 0.28 mm were used in this study. They were injected into bolus material (10 cm × 10 cm × 2 cm) with short and long types as shown in Fig. 1. These markers were pieces of gold wire that folded and collapsed during implantation under the pressure of the soft surrounding tissues. They were implanted according to the manufacturer's instructions with prepared application needles and were sandwiched by a Tough Water (TW) phantom (Kyoto Kagaku Co., Ltd., Kyoto, Japan). For the investigation of 4D modeling feasibility under various phantom thicknesses, the TW phantom was added at 2 cm intervals (in upper and lower each by 1 cm).

All markers were scanned with a computed tomography (CT) system (Optima CT 580W; GE Healthcare, Milwaukee, WI). Single-energy CT images were acquired according to standardized treatment-planning body protocol with 120 kV, 400 mA s, a 500 mm field of view (FOV), and slice thickness of 1.25 mm. The transversal pixel resolution was 0.977 mm. The CT scans were transferred to an iPlan RT Dose treatment planning system (TPS) version 4.5.3 (Brainlab AG, Feldkirchen, Germany). The virtual target was created by delineating the contour of the CT images for plan design. This plan was transferred to the Vero4DRT and ExacTrac systems (BrainLAB AG, Feldkirchen, Germany), and the implanted marker was defined by the planning CT on the ExacTrac system.

Fig. 2 shows a diagram of the experimental setup for investigating the feasibility of 4D-modeling. The programmable dynamic phantom (CIRS Inc., Norfolk, VA, USA), capable of producing motion based on an arbitrary input function, was used to simulate breathing-induced organ motion synchronously with a respiratory surrogate. This dynamic phantom had two tables: one that moved in the horizontal direction and one that moved in the vertical direction. The TW phantom with the fiducial markers was placed on the horizontal table. The phantom with five IR markers was placed on the vertical table to acquire a breathing signal. A sinusoidal motion wave sequence was produced in the dynamic phantom, using different amplitudes and breathing periods. The amplitude of the IR marker motion was fixed at 20 mm. A 3 s cycle was evaluated when the

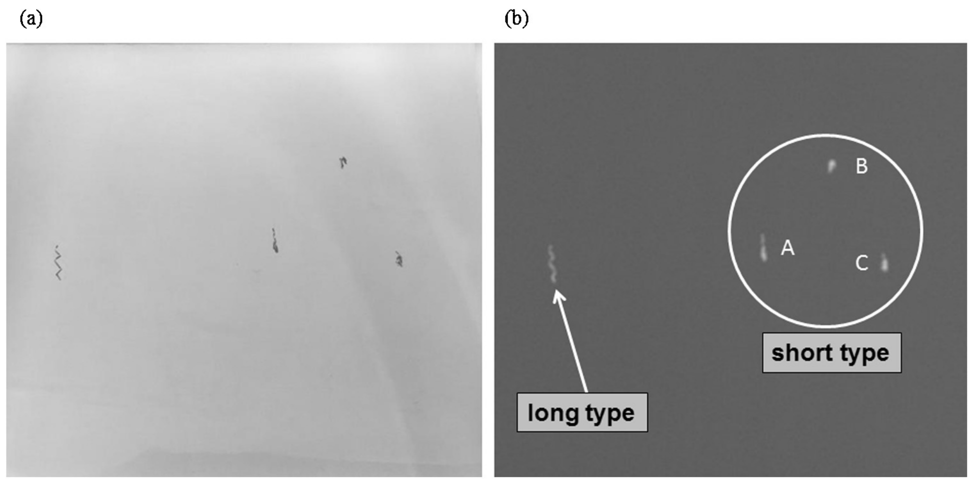

Fig. 1 – (a) Optical image and (b) kV planar image of bolus material with gold anchor markers. Short type markers were defined A, B and C as shown in the figure.

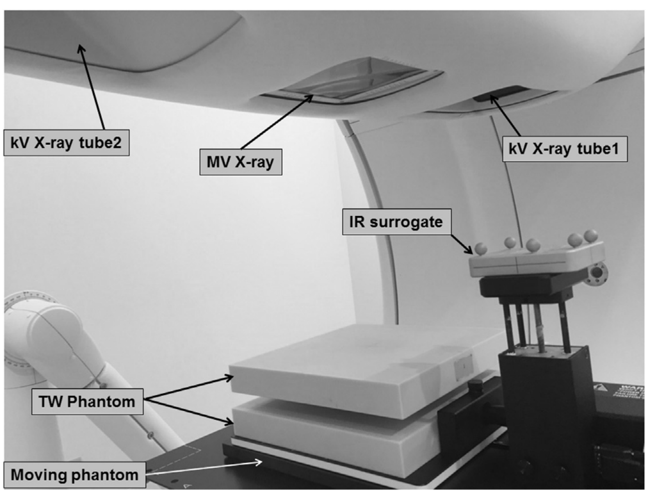

Fig. 2 – Diagram of the experimental setup for investigating the feasibility of 4D modeling.

amplitude of the target motion was fixed at 30 mm. The fiducial and IR surrogate markers were simultaneously acquired to calculate the 4D modeling function. A pair of orthogonal kV X-ray tubes was used at gantry angles of 45 and 315° to detect the fiducial markers. Therefore, the phantom of thickness of 10 cm had a water equivalent depth of 14.1 cm (10 × cos 45°). X-ray imaging parameters of 80 and 125 kV (320 mA and 5 ms) were used, respectively. Each image was extracted using the software IMAGEJ v1.49 (National Institutes of Health, Bethesda, MD). The statistical information of the marker and the background was used to calculate the contrast-to-noise ratio (CNR). The CNR is defined by:

$$\mathrm{CNR} = \frac{|S_M - S_B|}{\sigma_B}$$

where S_M is the maximum signal intensity produced by each gold anchor marker, S_B is the background signal intensity and σ_B is the standard deviation of the background noise. Each measurement was performed independently for each marker five times to get an average reading. The positions of the fiducial markers were detected using the orthogonal kV images acquired every 320 or 640 ms, and the intervals depended on the velocity of the markers. The IR camera on the ceiling treatment room monitored the surrogate IR markers every 16.7 ms. The ExacTrac system automatically calculated the 4D model after correlating the motion data of the fiducial and surrogate IR marker. The predicted target positions were calculated using the 4D modeling function, expressed by a quadratic equation involving two variables, in the ExacTrac system. The mean and standard deviation of the absolute difference between the detected and predicted target positions for 4D modeling were displayed on the screen of the Vero4DRT system. In clinical use, DTT can be performed after the 4D modeling process. We did not irradiate the dosimetric quality assurance (QA) device such as a film in this study, because several investigators reported a high tracking accuracy of DTT through using chamber and film measurements, even for rapidly moving patterns.[11–14] In addition, the difference between 4D modeling and dosimetric results is very small because the motions of the fiducial and surrogate IR markers are perfectly synchronized. The detected target and predicted target positional data were recorded in the ExacTrac log file. The log files were analyzed to estimate how often detection errors occurred during the 4D modeling process. We defined the detection error of the fiducial marker as the 4D modeling limitation. The 4D modeling process was attempted using short and long types. The exposure doses were collected using a real-time air ionization chamber (AccuGold, Radcal, Monrovia, CA) at the isocenter in air.

3. Results

Fig. 3 shows the kV planar images of the gold anchor markers on the various phantom thicknesses under 80 kV and 125 kV. The gold anchor markers in short and long types were well visualized in the images under 125 kV. However, these markers were not clearly visible with a phantom thickness of 10 cm under 80 kV. Fig. 4 shows the CNR of each gold anchor marker

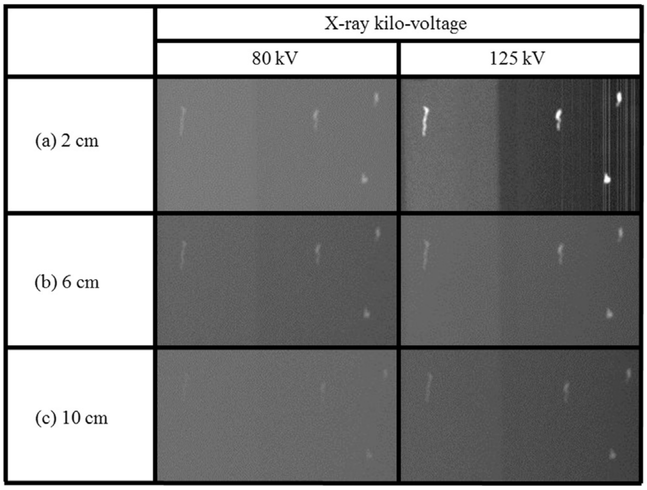

Fig. 3 – Gold anchor marker images under phantom thicknesses of (a) 2, (b) 6, and (c) 10 cm under 80 kV and 125 kV.

plotted as a function of phantom thickness. Image CNR of the short type marker was slightly higher than that of the long type one. The contrast for 6 cm and 10 cm of phantom thickness under 80 kV, the decrease was about 41% and 50% compared to the 2 cm phantom thickness, respectively. The contrast for 6 cm and 10 cm of phantom thickness under 125 kV, the decrease was about 71% and 78% compared to the 2 cm phantom thickness, respectively. Contrast of the gold anchor marker decreased as phantom thickness increased. Fig. 5 shows the predicted and detected target motions by 4D modeling on phantoms with 10 cm and 12 cm thicknesses under 125 kV. As shown, the gold anchor marker was sometimes not detected with a phantom thickness of more than 12 cm. This loss of detectability because of 4D modeling errors was found to be approximately 16% (5/31) with both types of marker. The 4D modeling limitation for both types was with a phantom thickness of 6 and 10 cm under 80 and 125 kV, respectively. However, the loss in detectability of the gold anchor marker because of 4D modeling errors was found to be approximately 6% (2/31) with a phantom thickness of 2 cm under 125 kV. 4D modeling could be performed except under the described conditions. The imaging dose from the orthogonal kV X-ray imaging subsystem was 0.18 mGy and 0.28 mGy per one shot under 80 kV and 125 kV, respectively.

4. Discussion

The fiducial marker for the purpose of 4D modeling in the Vero4DRT system should be awareness as marker. Meanwhile, large gold markers produce an extensive metal artifact on the planning CT image that interferes with structure delineation and dose calculations. To avoid these issues, the feasibility of 4D modeling using a gold anchor marker was investigated. Our

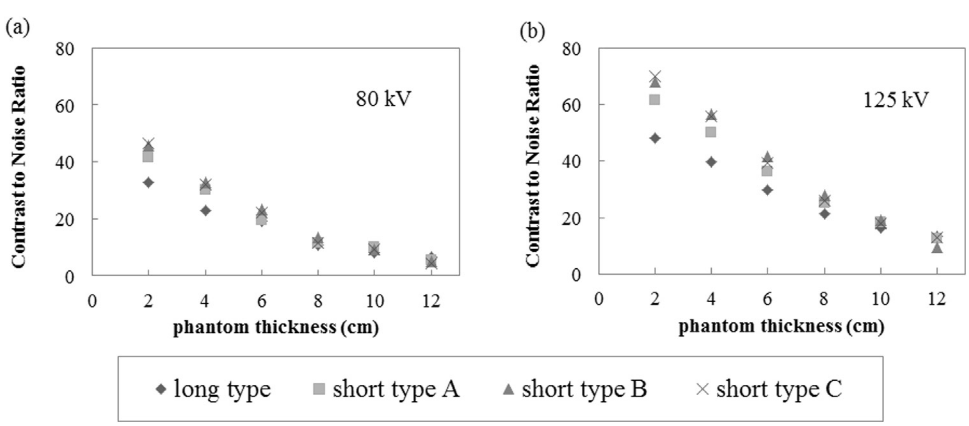

Fig. 4 – Contrast-to-noise ratio of each gold anchor marker as a function of phantom thickness at (a) 80 kV and (b) 125 kV.

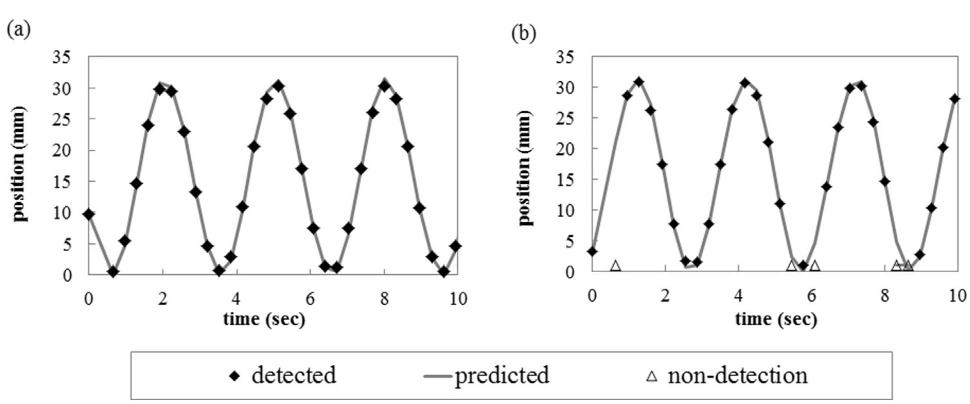

Fig. 5 – Graphs of detected and predicted target motions for water phantom thicknesses of (a) 10 and (b) 12 cm under 125 kV.

present phantom study of 4D modeling found that the gold anchor marker could be visualized under 125 kV. However, it was not clearly visible under more than approximately a phantom thickness of 10 cm because of poor image contrast under 80 kV. The contrast of gold anchor marker decreased as the phantom thickness increased. Thus, the kV setting required depends on patient thickness and treatment site. For thick phantoms, poor image contrast and high noise means that 4D modeling is inefficient because of poor detection capability. The gold anchor marker as short and long types was usable for DTT with a thin phantom. That is, gold anchor marker can be used with DTT for short water equivalent path length site, such as lung cancer patients. Application of the gold anchor marker for 4D modeling is difficult for abdominal region tumors such as in liver or pancreas cancer patients. We defined that the fiducial marker could not detect even at least one on as a 4D-modeling limitation. Actual patient respiratory systems are more complex than what was investigated in the present study. Gold anchor markers are flexible and curl up in a stable form at the parenchyma cells. The detection limited diameter of a fiducial marker as a short type is within 2 mm and as a long type it is within 20 mm, based on the information from the manufacturer. It should be noted that a gold anchor marker with a size exceeding the detection limitation cannot be detected by the ExacTrac system.

High contrast with the fiducial marker is needed for 4D modeling. Higher atomic number materials, such as gold using high kV settings, absorb more photons, leading to significant contrast enhancement. The imaging dose from orthogonal kV X-ray imaging subsystems have been shown to be 0.18 mGy and 0.28 mGy per one shot under 80 kV and 125 kV, thus being similar to previous reports.[10,11] Approximately 63 sets of kV images were required for the 4D modeling process at a pulse of 320 ms. The absorbed dose for the 4D modeling process is at least 11 mGy and 17 mGy per fraction under 80 and 125 kV, using two orthogonal sets of kV X-ray tubes. The radiation dose used should minimize any unnecessary exposure of the patients to radiation, based upon standard radiation safety principles “as low as reasonably achievable”.[15]

The respiratory pattern used in this work was rather simple. A finite state model of respiratory motion proposed by We et al.[16] should be examined to perform 4D modeling more reliably. The optimal X-ray monitoring angle for creating a 4D model should be investigated by considering that the intensity ratio of the gold markers decreases because of reduced radiation dose as they travel through tissues.[17] Gold anchor markers may be useful for follow-up CT scans to reduce metal artifacts[9] and for dose calculation to reduce a high atomic number volume.[5] Several important issues associated with the gold anchor markers for DTT using the Vero4DRT system include migration, deformation, and dose perturbations. These will need to be evaluated in further studies prior to clinical implementation.

5. Conclusions

Our phantom study is the first report on the feasibility of gold anchor markers in DTT using the Vero4DRT system. We found that a gold anchor marker with a length of 10 mm in a folded short type produced high contrast, indicating its applicability. The DTT feature of the Vero4DRT system performed well with the gold anchor marker under thin phantom thicknesses. It was shown that a gold anchor marker with a length of 10 mm in short and long types can be used with DTT for short water equivalent path length site, such as lung cancer patients, in the Vero4DRT system. However, we do not recommend using a gold anchor marker for abdominal region tumors, such as in liver or pancreas cancer patients because of poor contrast.

Conflict of interest

None.

Financial disclosure

No funding.

REFERENCES

1. Keall PJ, Mageras GS, Balter JM, et al. The management of respiratory motion in radiation oncology report of AAPM Task Group 76. *Med Phys* 2006;**33**:3874–900.
2. Matsuo Y, Ueki N, Takayama K, et al. Evaluation of dynamic tumor tracking radiotherapy with real-time monitoring for lung tumors using a gimbal mounted linac. *Radiother Oncol* 2014;**112**:360–4.
3. Matsuo Y, Verellen D, Poels K, et al. A multi-centre analysis of treatment procedures and error components in dynamic tumor tracking radiotherapy. *Radiother Oncol* 2015;**115**:412–8.
4. Depuydt T, Poels K, Verellen D, et al. Treating patients with real-time tumor tracking using the Vero gimbaled linac system: implementation and first review. *Radiother Oncol* 2014;**112**:343–51.
5. Chow JC, Grigorov GN. Dose measurements near a non-radioactive gold seed using radiographic film. *Phys Med Biol* 2005;**50**:N227–34.
6. Tanaka O, Iida T, Komeda H, et al. Initial experience of using an iron-containing fiducial marker for radiotherapy of prostate cancer: advantages in the visualization of markers in computed tomography and magnetic resonance imaging. *Pol J Med Phys Eng* 2016;**22**:91–4.
7. Chan MF, Cohen GN, Deasy JO. Qualitative evaluation of fiducial markers for radiotherapy imaging. *Technol Cancer Res Treat* 2015;**14**:298–304.
8. Handsfield LL, Yue NJ, Zhou J, et al. Determination of optimal fiducial marker across image-guided radiation therapy (IGRT) modalities: visibility and artifact analysis of gold, carbon, and polymer fiducial markers. *J Appl Clin Med Phys* 2012;**13**:3976.
9. Habermehl D, Henkner K, Ecker S, et al. Evaluation of different fiducial markers for image-guided radiotherapy and particle therapy. *J Radiat Res* 2013;**54**(Suppl. 1):i61–8.
10. Kamino Y, Takayama K, Kokubo M, et al. Development of a four-dimensional image-guided radiotherapy system with a gimbaled X-ray head. *Int J Radiat Oncol Biol Phys* 2006;**66**:271–8.
11. Takayama K, Mizowaki T, Kokubo M, et al. Initial validations for pursuing irradiation using a gimbals tracking system. *Radiother Oncol* 2009;**93**:45–9.
12. Miura H, Ozawa S, Tsuda S, et al. Quality assurance for dynamic tumor tracking using the Vero4DRT system. *Int J Cancer Ther Oncol* 2016;**4**:4112.
13. Ebe K, Sugimoto S, Utsunomiya S, et al. Development of a video image-based QA system for the positional accuracy of

dynamic tumor tracking irradiation in the Vero4DRT system. *Med Phys* 2015;**42**:4745–54.
14. Mukumoto N, Nakamura M, Sawada A, et al. Accuracy verification of infrared marker-based dynamic tumor-tracking irradiation using the gimbaled X-ray head of the Vero4DRT (MHI-TM2000). *Med Phys* 2013;**40**:041706.
15. NCRP. *Implementation of the principle of as low as reasonably achievable (ALARA) for medical and dental personnel, NCRP Report 107*; 1990.
16. Wu H, Sharp GC, Salzberg B, et al. A finite state model for respiratory motion analysis in image guided radiation therapy. *Phys Med Biol* 2004;**49**:5357–72.
17. Akimoto M, Nakamura M, Mukumoto N, et al. Optimization of the X-ray monitoring angle for creating a correlation model between internal and external respiratory signals. *Med Phys* 2012;**39**:6309–15.